Received: 27 June 2025 | Revised: 5 December 2025 | Accepted: 14 January 2026

DOI: 10.1002/pro.70488

RESEARCH ARTICLE

THE PROTEIN SOCIETY WILEY

The cytokinesis regulator RacGAP1 is a Rac1-specific GAP on membranes

Pavlina Dubois | Yann Ferrandez | Clara Rey | Cyril Pages | Agata Nawrotek | Jacqueline Cherfils

CNRS, Ecole Normale Superieure Paris-Saclay, Université Paris-Saclay, Gif-sur-Yvette, France

Correspondence
Agata Nawrotek and Jacqueline Cherfils, CNRS, Ecole Normale Superieure Paris-Saclay, Université Paris-Saclay, Gif-sur-Yvette, France.
Email: agata.maalouf@ens-paris-saclay.fr and jacqueline.cherfils@wanadoo.fr

Funding information
Académie des Sciences, Institut de France (Grand Prix Jungfleisch); Fondation pour la Recherche Médicale, Grant/Award Number: EQU202003010344; Agence Nationale de la Recherche, Grant/Award Numbers: ANR-18-0013-02, ANR-22-CE11-0004

Review Editor: Zengyi Chang

Abstract

Rho family small GTPases are essential for cytokinesis completion. RacGAP1, a dimeric multidomain protein with a lipid-binding C1 domain and a GTPase-activating protein (GAP) domain, is a major regulator in this process. However, despite many cellular and biochemical studies, whether RhoA or Rac1 is the actual substrate inactivated by RacGAP1 has remained a matter of debate. Rho family GTPases are inactivated by their GAPs on membranes, but the activity and specificity of RacGAP1 have only been studied biochemically in solution. Here, we reconstituted RacGAP1 in a membrane environment, using liposomes and highly purified proteins. Our study reveals that PS is a major lipid required for RacGAP1 membrane-binding in addition to PIP_2, and that the GAP domain cooperates with the C1 domain for membrane-binding. Consistently, fluorescence-based kinetics show that membranes potentiate the activity of RacGAP1 and of the C1GAP and GAP constructs towards Rac1. However, membranes do not modify RacGAP1 marked specificity for Rac1, identifying it as a Rac1-selective GAP. The Rac1-GDP-Pi crystal structure and mutagenesis identify the switch 1 and the insert region as important determinants for this specificity. Together, our results suggest a structural model in which the Rac1-RacGAP1 complex associates snugly with the membrane to efficiently remove Rac1 from the division plane.

KEYWORDS
cytokinesis, GTP hydrolysis, membrane, protein-membrane interaction, Rac1, RacGAP1, Rho GTPases, specificity

1 | INTRODUCTION

Cytokinesis, which occurs at the end of cell division, involves the formation of the cleavage furrow, which positions the division plane leading to daughter cells (reviewed in Wadsworth, 2021). A major regulator in this process is RacGAP1 (also known as MgcRacGAP, and called CYK-4 in *C. elegans*) (reviewed in White & Glotzer, 2012). RacGAP1 is also known as a subunit of centralspindlin, in which it forms a complex with the kinesin motor MKLP1 that is essential for the assembly of the mitotic spindle and the completion of cytokinesis (Mishima et al., 2002; Pavicic-Kaltenbrunner et al., 2007). RacGAP1 is a multidomain protein comprised of a dimeric N-terminal coiled coil region, where MKLP1 binds, a lipid-binding C1 domain and a GTPase-activating protein (GAP) domain that inactivates small GTPases of the Rho/Rac/Cdc42 subfamily, flanked by regions of

Pavlina Dubois and Yann Ferrandez have contributed equally to this study.

undefined structure (Jantsch-Plunger et al., 2000; Toure et al., 1998) (Figure 1a). The structures of the coiled-coil, C1 and GAP domains have been determined (Lekomtsev et al., 2012; Murayama et al., 2024; Pan et al., 2021). The C1 domain has a conventional diacylglycerol-binding C1 fold (Lekomtsev et al., 2012). However, it binds to phosphatidylinositol 4,5-bisphosphate (PIP_2) and phosphatidylinositol 4-phosphate (PI(4)P) phosphoinositides in vitro and is necessary for the association of RacGAP1 to the plasma membrane, suggesting that its role is to link the mitotic spindle to the plasma membrane by binding to these lipids (Lekomtsev et al., 2012). The structures of the GAP domain in complex with Cdc42 or fused to RhoA carrying a phosphomimetics, both bound to GDP and the transition state phosphate analog AlF_3 (Murayama et al., 2024), showed that the GAP domain is highly similar to that of conventional GAPs which inactivate small GTPases of the Rho/Rac/Cdc42 subfamily by stimulating the hydrolysis of GTP into GDP (reviewed in Cherfils & Zeghouf, 2013). In particular, the GAP domain features a conserved arginine ("the Arg finger") which points into the GTP-binding site, as observed in structures of related RhoGAP/Rho GTPase complexes where it is critical for GTP hydrolysis (Rittinger et al., 1997). Accordingly, mutation of the Arg finger in RacGAP1 produces a GAP-dead mutant that is unable to support cytokinesis completion, which underlines the functional importance of the GAP-stimulated reaction (Canman et al., 2008; Miller & Bement, 2009; Zhang & Glotzer, 2015).

However, the identity of the actual substrate of RacGAP1 has remained a matter of debate despite many in vitro, cellular and genetics studies (reviewed in Basant & Glotzer, 2017). The Rho GTPases subfamily, of which RhoA, Rac1 and Cdc42 are the most studied, are major regulators of cell shape and motility (reviewed in Jaffe & Hall, 2005). Notably, RhoA is a major regulator of cytokinesis and is enriched at the cleavage furrow (reviewed in White & Glotzer, 2012; Basant & Glotzer, 2017), while Rac1 is depleted from this region (Yoshizaki et al., 2003). Genetics studies in xenopus embryos and *C. elegans* favored RhoA as being the primary substrate of RacGAP1, which would lead to a flux in which RhoA is repeatedly activated by its guanine nucleotide exchange factor (GEF) ECT2 and inactivated by RacGAP1 (Miller & Bement, 2009; Zhang & Glotzer, 2015). In contrast, other studies proposed that the primary role of RacGAP1 is to inactivate Rac1. These included alternative genetic studies in xenopus embryos and in *C. elegans* (Canman et al., 2008; Zhuravlev et al., 2017), and in vitro biochemical studies of the activity of the GAP domain (Amin et al., 2016; Kawashima et al., 2000; Toure et al., 1998) or of full-length human RacGAP1 (Bastos et al., 2012), which found that RacGAP1 has GAP

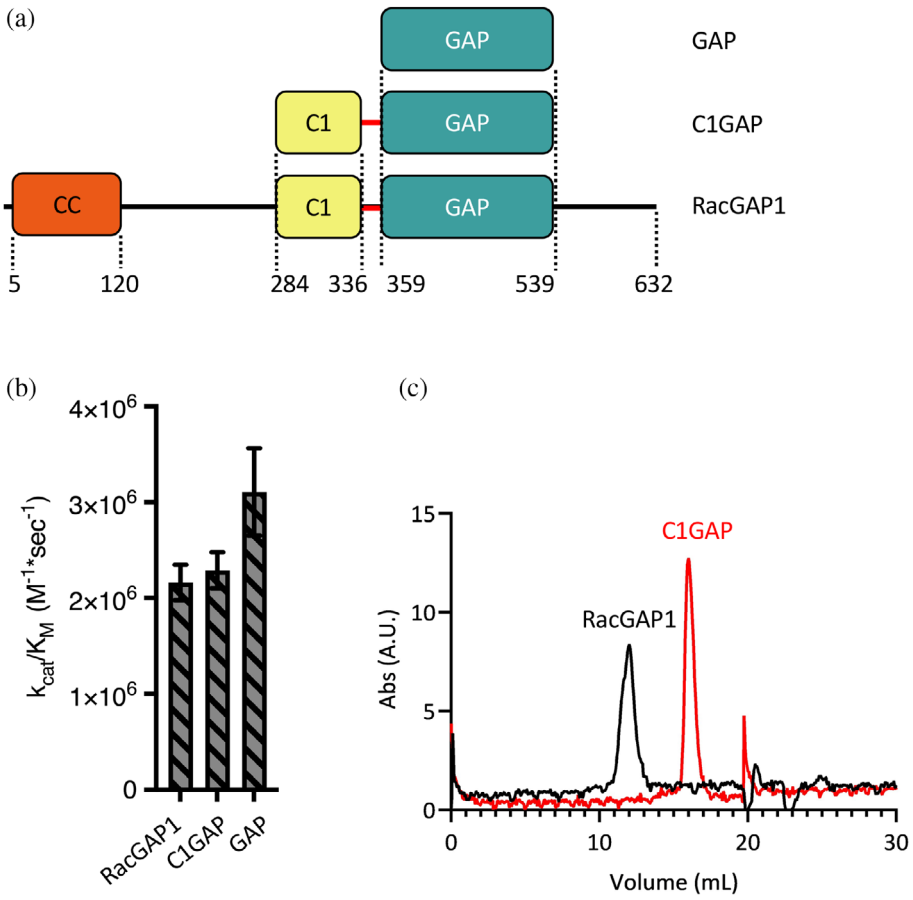

FIGURE 1 RacGAP1 is not autoinhibited in solution. (a) Schematic representation of the constructs used in this study. (b) Catalytic efficiency (k_{cat}/K_M) in solution, determined by fluorescence kinetics. k_{cat}/K_M were obtained from apparent rate constants (k_{obs}) determined over a range of GAP active site concentrations (0–20 nM). Bars represent the mean ± SD from 3 to 4 independent experiments. Statistical analysis is given in Table S1. (c) Oligomerization of RacGAP1 and C1GAP assessed by size-exclusion chromatography. The elution profile of RacGAP1 (black) corresponds to an estimated molecular weight of ~150 kDa, consistent with a dimer. The C1GAP construct (red) elutes at a volume consistent with a monomer (~25 kDa).

activity towards Rac1 and to a lesser extent Cdc42, but has no activity towards RhoA. These conflicting results underline the need for biochemical characterization that fully reflects physiological conditions.

A mechanism to solve this conundrum could be that determinants exist that control the specificity and/or the efficiency of RacGAP1. An earlier model proposed that phosphorylation of the GAP domain by the Aurora kinase would switch its specificity (Minoshima et al., 2003), however this mechanism was subsequentially ruled out (Bastos et al., 2012). In addition, phosphomimetics of the phosphorylation site did not enhance the activity towards Cdc42 or RhoA (Murayama et al., 2024). An alternative mechanism could be that the specificity of RacGAP1 is regulated by membranes. Indeed, most GAP reactions take place at the surface of membranes, to which activated Rho GTPases are reversibly associated by their lipidated C-terminus. Accordingly, membranes are increasingly recognized as major components of the regulation of the small GTPase cycle (reviewed in Cherfils & Zeghouf, 2013). Notably, membranes have been shown to potentiate the activity of GAPs for Arf GTPases (Bigay et al., 2003; Duellberg et al., 2021), Rab GTPases (Fullbrunn et al., 2024) and Rho GTPases (Karimzadeh et al., 2012). However, the GAP activity of RacGAP1 has not been studied in a membrane context. Here, we studied the activity and specificity of human RacGAP1 towards the three major Rho GTPases in a membrane environment, using liposomes and highly purified proteins, fluorescence-based kinetic assays, mutagenesis and X-ray crystallography. Our study reveals that, in addition to C1 domain-PIP_2 interactions, RacGAP1 forms non-specific interactions with phosphatidylserine (PS) through its GAP domain, and that membranes potentiate its activity towards Rac1. However, membranes do not modify its marked specificity towards Rac1, thus defining RacGAP1 as a Rac1-selective GAP on membranes. Using crystallography and mutagenesis, we identify the switch 1 and the insert region of Rac1 as important determinants of this specificity. Our results are consistent with a model in which the Rac1-RacGAP1 complex associates snugly with the membrane to efficiently remove Rac1 from the division plane.

2 | RESULTS

2.1 | Full-length RacGAP1 is not autoinhibited in solution

Earlier activity and specificity biochemical studies of RacGAP1 were carried out in solution, using the isolated GAP domain and/or non-quantitative assays. We therefore first characterized the activity of purified recombinant full-length RacGAP1 (RacGAP1 hereafter) towards Rac1 (Figures 1a and S1a), using a fluorescently labeled bacterial phosphate-binding sensor, which allows to quantify the GAP activity by measuring the kinetics of inorganic phosphate (Pi) release using fluorescence detection (Galicia et al., 2019; Mishra & Lambright, 2021; Nixon et al., 1995). The GAP rates were measured over a range of RacGAP1 concentrations, from which k_{cat}/K_M values were determined (Figures 1B and S1b, c). RacGAP1 displayed a k_{cat}/K_M of 2.2×10^6 M^{-1} s^{-1}, confirming that it is an efficient GAP for Rac1 and showing that it is not autoinhibited in solution (Bastos et al., 2012). We then analyzed whether dimerization of RacGAP1 contributes to its GAP activity, using a RacGAP1 construct that lacks the dimerization N-terminal coiled-coil and the C-terminal region beyond the GAP domain (C1 and GAP domains, C1GAP hereafter) (Figures 1a and S1a). Size exclusion chromatography (SEC) confirmed that RacGAP1 is dimeric and C1GAP monomeric (Figure 1c). C1GAP was equally active as RacGAP1 ($k_{cat}/K_M = 2.3 \times 10^6$ M^{-1} s^{-1}) (Figure 1b and S1d), indicating that in solution, the GAP activity towards Rac1 is not modulated by dimerization. Finally, the GAP domain alone was slightly more active than RacGAP1 and C1GAP ($k_{cat}/K_M = 3.0 \times 10^6$ M^{-1} s^{-1}), indicating that the C1 domain has only a small contribution, if any, to the regulation of the GAP activity in solution. Thus, RacGAP1 is an active GAP for Rac1 in solution, and neither the coiled-coil, C1 domain, or C-terminal region significantly modulate its GAP activity.

2.2 | Dissection of RacGAP1 interactions with negatively charged membranes

It was previously shown that the C1 domain binds to PIP_2 in vitro using liposomes, surface plasmon resonance, and in cells using PIP_2 depletion (Lekomtsev et al., 2012). To characterize further the role of negatively charged lipids in RacGAP1 binding to membranes, we carried out liposome flotations using liposomes of controlled lipid composition and size (Figures 2a and S2a and Table S2). As a control, RacGAP1 did not interact with neutral liposomes. RacGAP1 interacted strongly with liposomes containing 2% PIP_2 and 10% PS, which approximates the concentration of these lipids in the plasma membrane (about 70% of protein bound). Surprisingly, RacGAP1 interacted only weakly with liposomes containing 2% PIP_2 as the sole negatively charged lipids (22% bound), while a stronger interaction was observed with liposomes containing only PS (50% bound). These results suggest that PS is the primary lipid responsible for the interaction of RacGAP1 with membranes and that optimal binding requires both PS and PIP_2. The PS/PIP_2 liposomes (referred to as PML liposomes hereafter) were therefore used for subsequent experiments.

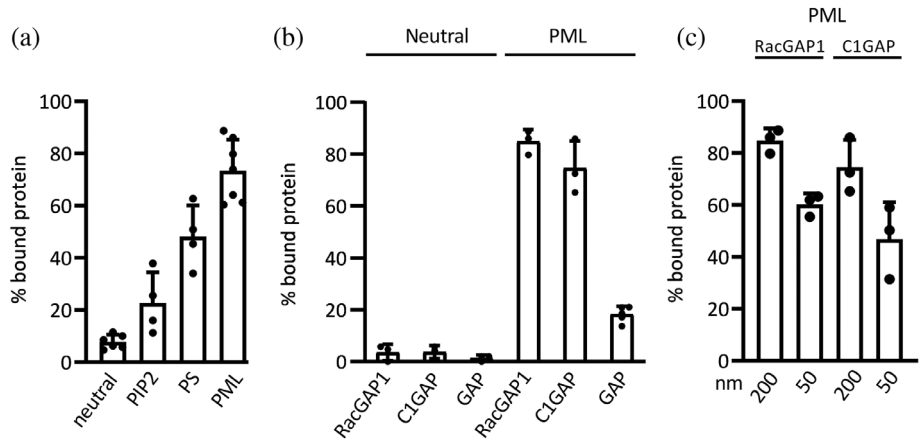

FIGURE 2 RacGAP1 uses both its GAP and C1 domains to bind to negatively charged liposomes. (a) Binding of RacGAP1 to neutral liposomes or to liposomes containing 2% PIP_2, 10% PS, or 2% PIP and 10% PS (PML liposomes). Binding was measured by flotation using 200 nm diameter liposomes. (b) Binding of RacGAP1, C1GAP, and the GAP domain to neutral or anionic PML liposomes (200 nm diameter). (c) Binding of RacGAP1 and C1GAP to large (200 nm diameter) or curved (50 nm diameter) PML liposomes. Bars represent mean ± SD from 2 to 4 independent experiments. Statistical analysis is in Table S1.

The contribution of PS to RacGAP1 binding to membranes suggests that RacGAP1 could form non-specific electrostatic interactions outside the C1 domain. To address this question, we compared the interaction of RacGAP1 with PML liposomes to those of C1GAP and of the GAP domain alone (Figures 2b and S2b). As a control, none of the truncated constructs interacted with neutral liposomes. C1GAP bound to PML liposomes as strongly as RacGAP1 (80%), suggesting that the N- and C-terminal regions do not contribute to the interaction of RacGAP1 with membranes. Surprisingly, the GAP domain alone displayed a weak interaction with PML liposomes (20%). Thus, binding of RacGAP1 to membrane involves the GAP domain in addition to the C1 domain, likely through non-specific interaction with anionic lipids.

RacGAP1 is dimeric, hence has twice the number of membrane-binding regions as C1GAP, which is monomeric. It is thus surprising that RacGAP1 does not bind to membranes more strongly than C1GAP. One explanation could be that, as a consequence of their different organizations and shapes, RacGAP1, but not C1GAP, is sensitive to membrane curvature. We assessed this possibility by comparing the binding of RacGAP1 and C1GAP to large liposomes (200 nm) and to smaller, curved liposomes (50 nm) (Figures 2c and S2c). RacGAP1 bound slightly less well to curved liposomes (60% bound); however, a similar decrease in binding was also observed for monomeric C1GAP (48% bound). Thus, while RacGAP1 has a slight preference for flat over curved membranes, this sensitivity is not due to its dimeric structure.

Together, our results show that while PIP_2 is needed for optimal binding of RacGAP1 to membranes, the primary phospholipid responsible for membrane binding is PS. Unexpectedly, the GAP domain binds to the membrane in addition to the C1 domain, and dimerization does not play a role in membrane-binding.

2.3 | RacGAP1 activity towards Rac1 is potentiated by negatively charged membranes

Since RacGAP1 interacts strongly with membranes, we next asked whether membranes affect its GAP activity. Rac1-GTP, the substrate of RacGAP1, is associated with membranes by its lipidated polybasic C-terminus. We showed previously in related GEF assays that a Rac1 construct carrying a polyhistidine tag in the C-terminus, which recruits it to Ni lipid-containing liposomes, is a fully functional surrogate of lipidated Rac1 (Ferrandez et al., 2017; Peurois et al., 2017). GAP kinetics in the presence of PML liposomes were performed with this Rac1 construct using the phosphate-sensor assay, which we optimized for use with liposomes by careful removal of Pi contamination prior to kinetics measurements (see methods). RacGAP1 displayed a 5-fold increase in activity towards Rac1 in the presence of membranes ($k_{cat}/K_M = 11.4 \times 10^6\ M^{-1}\ s^{-1}$), indicating that membranes potentiate its activity (Figures 3 and S3a,b). To assess whether dimerization contributes to this effect, the same experiment was carried out with the monomeric C1GAP construct. Surprisingly, membranes had a larger effect on the activity of C1GAP (21-fold increase, $k_{cat}/K_M = 40 \times 10^6\ M^{-1}\ s^{-1}$) (Figures 3 and S3c), resulting in an activity 4-fold higher than that of RacGAP1. Finally, membranes also increased the GAP activity of the isolated GAP domain, although to a slightly lesser extent (3-fold, $k_{cat}/K_M = 9.3 \times 10^6\ M^{-1}\ s^{-1}$) (Figures 3 and S3d, e).

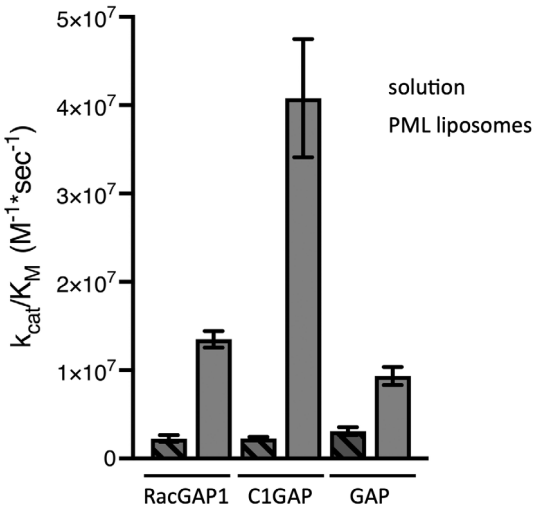

FIGURE 3 Anionic membranes potentiate the GAP activity of RacGAP1 towards Rac1. The catalytic efficiency of RacGAP1, C1GAP and GAP constructs was determined using fluorescence kinetics in solution (hatched bars) and on PML liposomes (gray bars). k_{cat}/K_M values were determined from k_{obs} obtained over a range of active sites concentrations (0 to 20 nM). Bars represent means ± SD of 3 independent experiments. Statistical analysis is in Table S1.

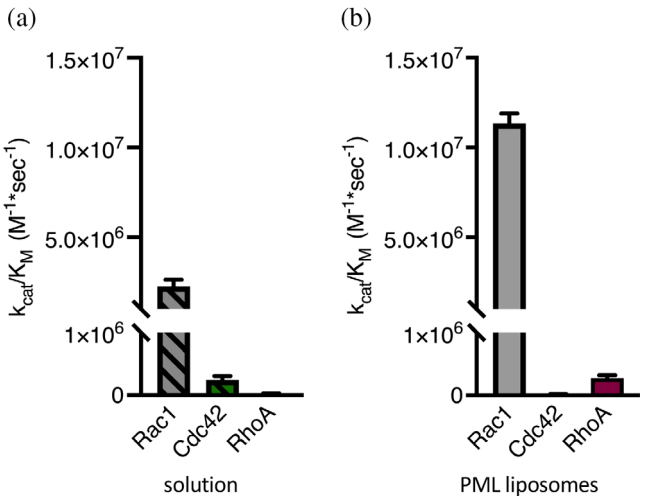

FIGURE 4 RacGAP1 is specific for Rac1 in solution and on membranes. (a) Catalytic efficiency in solution of RacGAP1 towards Rac1 (gray), Cdc42 (green), and RhoA (purple). (b) Catalytic efficiency on PML liposomes of RacGAP1 towards Rac1 and RhoA. No activity was observed towards Cdc42. All GTPases are attached to liposomes by their C-terminal His-tag. k_{cat}/K_M values were determined from k_{obs} obtained over a range of active site concentrations (0 to 50 nM). Bars represent means ± SD of 3–4 independent experiments. Statistical analysis is in Table S1.

Thus, membranes potentiate the GAP activity of RacGAP1, C1GAP, and the isolated GAP domain towards Rac1, with the largest activity increase seen for C1GAP, which is consistent with their membrane-binding properties.

2.4 | RacGAP1 is highly selective for Rac1 on membranes

Whether Rac1, Cdc42, or RhoA is the physiological substrate of RacGAP1 during cytokinesis has remained a matter of debate. The effect of membranes on the GAP activity of RacGAP1 towards Rac1 raises the possibility that membranes could also modulate its specificity, an effect that was previously observed for a GEF for Arf GTPases (Padovani et al., 2014). To investigate this possibility, we determined the efficiency of RacGAP1 towards RhoA and Cdc42 on membranes. As a reference, we first determined the GAP efficiency of RacGAP1 in solution towards each GTPase (Figures 4a and S4a). Although a weak GAP activity could be measured towards Cdc42 ($k_{cat}/K_M = 0.24 \times 10^6$ M^{-1} s^{-1}) and RhoA ($k_{cat}/K_M = 0.025 \times 10^6$ M^{-1} s^{-1}), this activity was 9 times (Cdc42) and 88 times (RhoA) weaker than that towards Rac1 ($k_{cat}/K_M = 2.2 \times 10^6$ M^{-1} s^{-1}). These results confirm the weak activities in solution previously reported in (Bastos et al., 2012). Next, we measured the GAP activity of RacGAP1 towards these small GTPases in the presence of PML liposomes (Figure 4b and S4b). All GTPases were attached to PML liposomes containing Ni-lipids by their C-terminal His-tag (Peurois et al., 2017). An even smaller activity was measured towards Cdc42 ($k_{cat}/K_M = 0.093 \times 10^6$ M^{-1} s^{-1}, about 2-fold decrease, 122 times lower than Rac1). PML liposomes stimulated the GAP activity of RacGAP1 towards RhoA by 11-fold ($k_{cat}/K_M = 0.28 \times 10^6$ M^{-1} s^{-1}), but this activity remained considerably lower (41 times) than that towards Rac1 ($k_{cat}/K_M = 11.4 \times 10^6$ M^{-1} s^{-1}).

We conclude that membrane-bound RacGAP1 has a marked specificity for Rac1 over RhoA and Cdc42, hence that membranes do not function as specificity modulators for RacGAP1.

2.5 | The Rac1-GDP-Pi structure suggests that the Pi release step contributes to RacGAP1 specificity

The specificity of RacGAP1 for Rac1 may stem from structural differences between Rac1 and other Rho-family GTPases that could be detected by RacGAP1 in the course of the GAP reaction. Structures of Rac-GTP (substrate) (Hirshberg et al., 1997; Krauthammer et al., 2012), Rac1-GDP-AlF_3 (transition state, determined in complex with bacterial GAPs) (Stebbins & Galan, 2000; Wurtele et al., 2001), and Rac1-GDP (product) (Ferrandez et al., 2017, this study) along the GTP hydrolysis reaction have been determined. To complete the GTP hydrolysis structural pathway, we determined a high-resolution crystal structure of Rac1-GDP-Pi, the intermediate that follows the

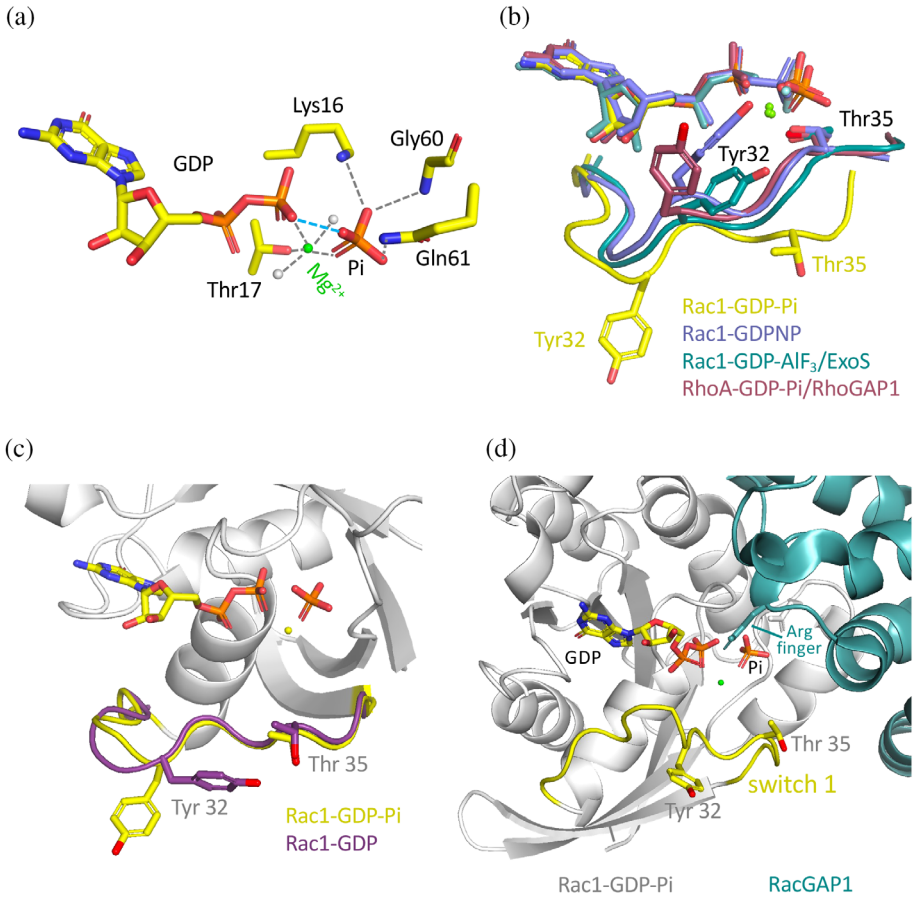

FIGURE 5 Crystal structure of Rac1-GDP-Pi. (a) Close-up view of the catalytic site of Rac1 around GDP-Pi. The Mg^{2+} ion is in green, surrounding water molecules in gray. Residues that interact with Mg^{2+} or Pi are shown. Hydrogen bonds are in dashed lines. (b) The closed (GDPNP, GDP-AlF_3) and open (GDP-Pi) conformations of the switch 1 of Rac1 along the GTP hydrolysis reaction. The closed conformation of RhoA-GDP-Pi in complex with RacGAP is shown for comparison. PDB entries: Rac1GDPNP, PDB ID: 3TH5; Rac1-GDP-AlF3, PDB ID: 1HE1; RhoA-GDP-Pi/RhoGAP, PDB ID: 6R3V. (c) The switch 1 in Rac-GDP-Pi is in the open conformation as Rac-GDP. Note that it lacks interactions of Tyr32 and Thr35 with the bound nucleotide. Rac1-GDP is from this study. (d) The open conformation of the switch 1 in Rac1-GDP-Pi is compatible with its interaction with RacGAP1. Rac1-GDP-Pi is overlaid onto Cdc42 from the Cdc42-GDP-AlF_3/RacGAP1 complex (PDB ID: 5C2J).

transition state and precedes the dissociation of the GDP and Pi products (Figures 5a and S5a and Table S3). The structure shows that the positions of the GDP and Pi ligands in the nucleotide-binding pocket are similar to those previously observed in such intermediates, including unbound Rab11-GDP-Pi (Pasqualato & Cherfils, 2005), SOS-bound Ras-GDP-Pi (Sondermann et al., 2004), and RhoA-GDP-Pi bound to RhoGAP (Molt Jr. et al., 2019) (Figure S5b). Notably, the catalytic Gln61 in the switch 2 has a canonical position, and one oxygen of Pi is located within hydrogen bonding distance (2.6 Å) of the leaving oxygen of GDP. These observations suggest that Rac1 follows the canonical catalytic mechanism, possibly involving substrate-assisted hydrolysis as proposed for Rab11 (Pasqualato & Cherfils, 2005).

However, the switch 1 of Rac1-GDP-Pi is remote from the nucleotide-binding site (referred to as open conformation), in contrast with that of RhoA in the RhoA-GDP-Pi-RhoGAP1 complex (Molt Jr. et al., 2019) (referred to as closed conformation) (Figure 5b). Rac1-GTP (Hirshberg et al., 1997; Krauthammer et al., 2012) and Rac1-GDP-AlF_3 bound to bacterial GAPs (Stebbins & Galan, 2000; Wurtele et al., 2001) also display a closed conformation (Figure 5b). In contrast, the open conformation is seen in Rac1-GDP (Ferrandez et al., 2017, this study) (Figure 5c). Compared to the closed conformation, the open conformation lacks major interactions with the bound nucleotide, including the interaction of Thr35 with Mg^{2+}, and Tyr 32 points outside rather than towards the nucleotide-binding site and does not interact, directly or through a water molecule, with the γ-phosphate. Importantly, overlay of Rac1-GDP-Pi with the Cdc42-RacGAP1 and RhoA-RacGAP1 complexes (Murayama et al., 2024) shows that Rac1-GDP-Pi is compatible with the interaction with RacGAP1 (Figure 5d), suggesting that the switch 1 may convert to the open conformation at the Rac1-GDP-Pi intermediate while still bound to RacGAP1. The absence of interaction of Pi with the switch 1 could then facilitate Pi release, and Rac1-GDP could dissociate from RacGAP1 without further conformational change. Together, the structure of Rac1-GDP-Pi points to a dynamical determinant at the switch 1 that could be perceived by RacGAP1 at the Pi release step.

2.6 | The switch 1 and the insert helix contribute to RacGAP1 specificity towards Rac1

Next, we searched for sequence differences between Rac1 and RhoA/Cdc42 that could contribute to the

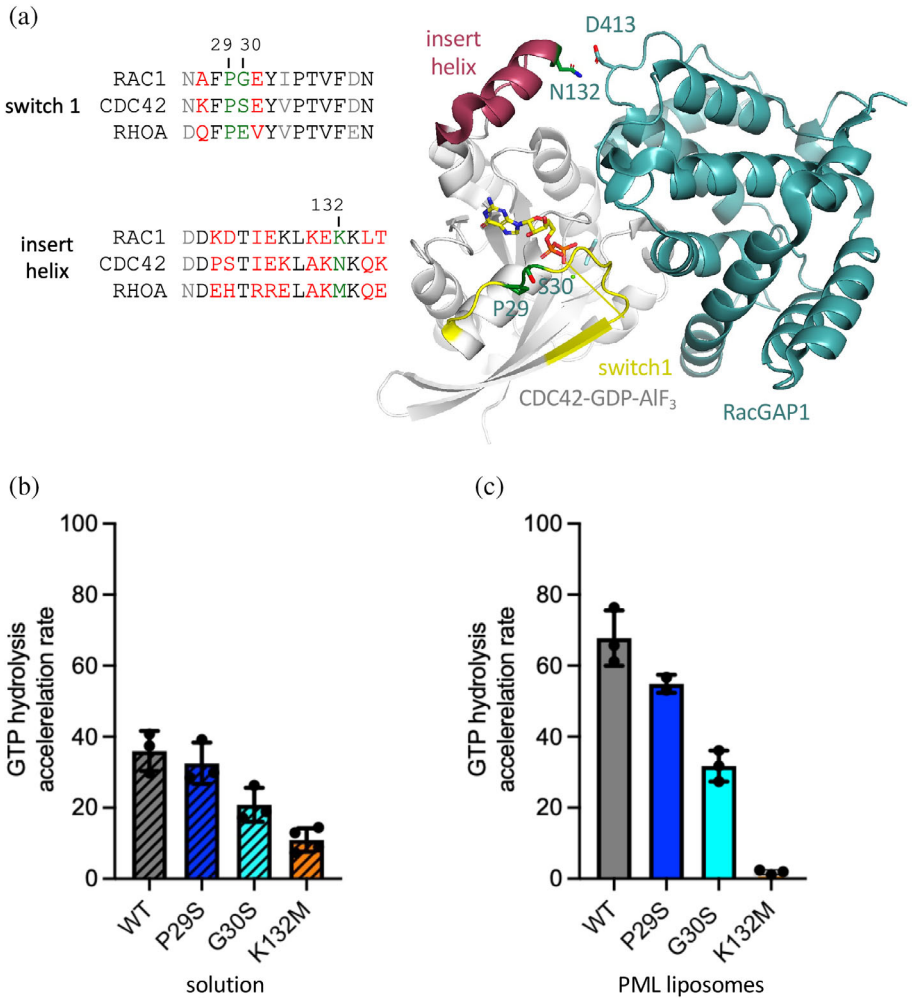

FIGURE 6 Determinants of the specificity of RacGAP1 for Rac1. (a) Left: Sequence alignment of the switch 1 and insert helix of Rac1, RhoA, and Cdc42. Conservative changes are in gray, non-conserved residues in red, and residues mutated in this study in green. Right: Position of the residues mutated in Rac1, shown on the structure of the Cdc42–RacGAP1 complex (PDB ID: 5C2J). (b) Acceleration of the rate of inactivation of Rac1 mutants by RacGAP1 in solution. (c) Acceleration of the rate of inactivation of Rac1 mutants by RacGAP1 with PML liposomes. Bars represent mean ± SD from three independent experiments. Statistical analysis is in Table S1.

specificity of RacGAP1 for Rac1. First, we located an appealing difference in the switch 1, Gly30, an amino acid that uniquely provides flexibility to proteins. This residue is replaced by Ser in Cdc42 and Glu in RhoA (Figure 6a). We mutated Gly30 to Ser, as found in Cdc42, which resulted in a 2-fold decrease of the GAP activity of RacGAP1 both in solution and in the presence of PML liposomes (Figure 6b,c). Since residues at this position do not contact GAP domains in any of the known structures of Rho family GTPase/GAP complexes, it is likely that the mutation propagates structural differences elsewhere in the switch 1, probably by reducing the flexibility of the switch 1. Interestingly, a Pro29Ser Rac1 mutation, a conserved residue located next to Gly30 (Figure 6a) was found in human melanoma (Krauthammer et al., 2012), which may also modify the flexibility of the switch 1 and affect the GAP reaction. However, the Pro29Ser mutation had no effect on the activity of RacGAP1 (Figure 6b,c), indicating that the physiological effect of the mutation at Pro29 does not arise from a defect in its sensitivity to RacGAP1.

The replacement of Gly30 in Rac1 by other residues in Cdc42 and RhoA is not sufficient to account for the large drop in efficiency of RacGAP1 towards Cdc42 and RhoA. The crystal structures of RhoA and Cdc42 bound to GDP-AlF_3 and RacGAP1 (PDB ID: 5C2K and 5C2J) display a contact between Met132 (RhoA) or Asn132 (Cdc42) in the insert helix with Asp413 in the GAP domain (Figure 6a). Residue 132 is changed to Lys in Rac1, hence it may contribute to a specific Rac1/RacGAP1 interaction. Mutation of Lys132 to Met reduced the efficiency of RacGAP1 by 5-fold in solution, indicating that the insert contributes to Rac1/RacGAP1 interaction (Figure 6b). Surprisingly, this decrease was markedly stronger in the presence of PML liposomes (31-fold), suggesting that this residue could also be involved in the interaction of the Rac1/RacGAP1 complex with membranes (Figure 6c).

Taken together, our data suggest that the dynamics of the switch 1 encoded by Gly30 and the contact of the insert helix with RacGAP1 and possibly with the membrane are important determinants of the specificity of RacGAP1 for Rac1.

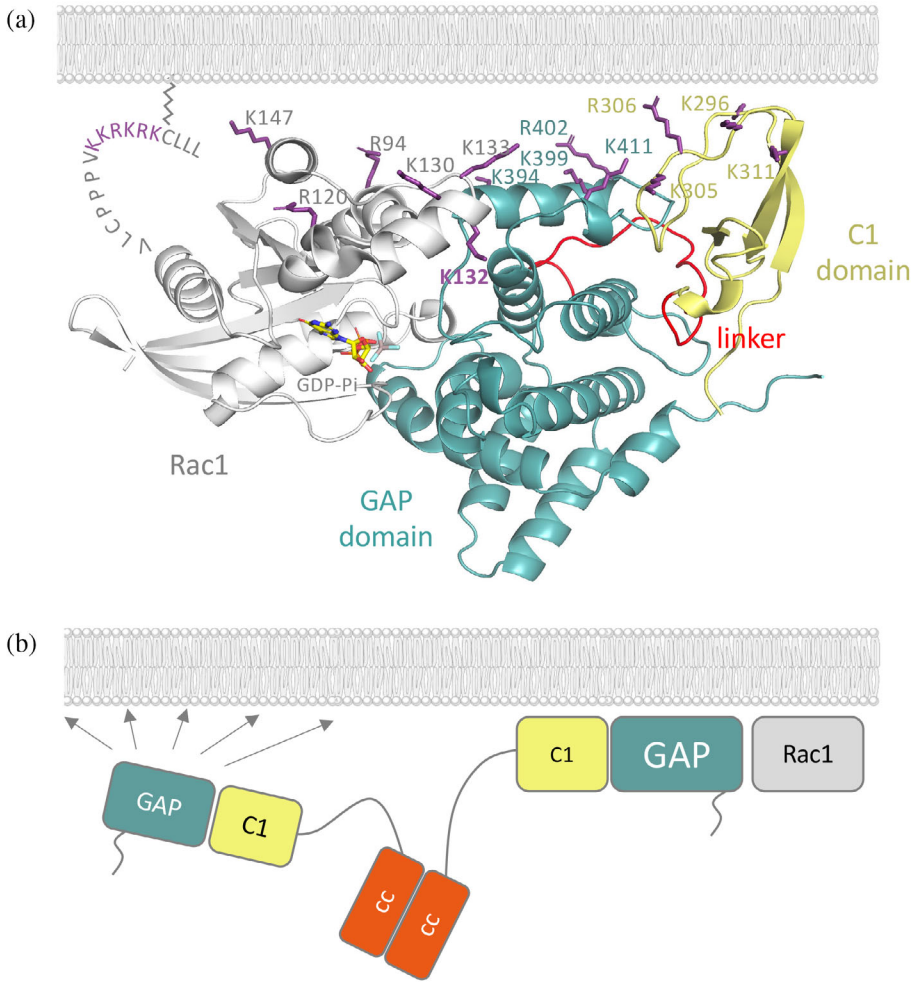

FIGURE 7 Model of the Rac1-RacGAP1 complex associated with membranes. (a) The Rac1-RacGAP1 model displays a positively charged surface oriented towards the membrane. The structure of C1GAP was generated by Alphafold 3, then the Rac1-C1GAP complex was oriented on the membrane by PPM/OPM. Arg and Lys residues facing the membrane are in violet. The position of the geranylgeranylated polybasic C-terminus of Rac1 is indicated. (b) Model of asymmetric binding of dimeric RacGAP1 to membranes. The unbound subunit (left) is free to search a large membrane surface for new Rac1-GTP substrates (arrows).

3 | DISCUSSION

In this study, we investigated how membranes affect the specificity and activity of RacGAP1 using in vitro reconstitutions, crystallography and mutagenesis. We found that PS is a major lipid needed for RacGAP1 binding to membranes, while PIP_2 is required for optimal binding. Our data show that the GAP domain, presumably through non-specific interactions with anionic lipids, cooperates with the C1 domain, previously reported to bind PIP_2 (Lekomtsev et al., 2012). Accordingly, the GAP activities towards Rac1 of full-length RacGAP1, of the C1GAP construct and of the GAP domain alone are stimulated by PIP_2/PS-containing membranes. Surprisingly, the C1GAP domain binds to membranes as well as full-length RacGAP, and is more active, pointing to a non-trivial negative role of dimerization by the N-terminal coiled-coil domain. However, membranes do not modify the marked specificity of RacGAP1 for Rac1. Finally, structural and mutagenesis analyses identify important determinants for this specificity, located in the switch 1 and the insert region of Rac1.

3.1 | The role of membranes in the inactivation of Rac1 by RacGAP1

These results provide important novel insight into the interaction of RacGAP1 with membranes and the role of membranes in Rac1 inactivation. AlphaFold predicts that the C1 and GAP domains of RacGAP1 form a compact unit in which the C1 domain is available for binding to the membrane and the GAP domain for binding Rac1 (Figure S6a). We used the AlphaFold C1GAP model and the structures of the GAP domain of RacGAP1 bound to Cdc42 and RhoA (PDB ID: 5C2K and PDB ID: 5C2J) to build a model of the Rac1/C1GAP complex, which we then docked to the membrane using the PPM/ server (Figure 7a). As a validation criterion, the known membrane-binding regions of Rac1 (geranylgeranylated polybasic C-terminus) and of RacGAP1 (PIP_2-binding site in the C1 domain) are oriented towards the membrane in the docked model. The model also places the GAP domain of RacGAP1 and the K132 residue in the insert region of Rac1 close to the membrane, in agreement with our membrane-binding and GAP activity results. Remarkably, the Rac1/RacGAP1 model displays a large polybasic

surface apposed to the membrane, comprised of multiple Lys and Arg residues on the C1 and GAP domains and on the GTPase core of Rac1 (Figure 7a). This positively charged tract is well suited to form multiple non-specific interactions with anionic lipids, in agreement with the recruitment of RacGAP1 to PS lipids and the sensitivity of its GAP domain to anionic membranes. Together, based on our biochemical and modeling data, we propose a mechanism of inactivation of Rac1 by RacGAP1 on membranes in which the Rac1/RacGAP1 complex apposes snugly on the membrane through multiple non-specific interactions of the Rac1 and C1GAP polybasic surfaces with anionic lipids, in addition to the previously described specific interactions of the C1 domain with PIP_2 (Lekomtsev et al., 2012). This points to an important role of the membrane in defining precisely the positions and orientations of Rac1-GTP and of the GAP domain, which allows their coincidence detection and productive interaction.

Of note, the arrangement of the C1 and GAP domains predicted for RacGAP1 is distinct from that of the related C1 and GAP domains of β2-chimaerin, which displays an autoinhibitory conformation in which the C1-GAP linker blocks access to the membrane-binding pocket of the C1 domain (Figure S6b) (Canagarajah et al., 2004). While co-localization of RacGAP1 and Rac1-GTP on the membrane is in principle sufficient to stimulate the efficiency of the GTPase reaction in itself (reviewed in Nawrotek et al., 2023), the autoinhibited β2-chimaerin structure raises the possibility that RacGAP1 could exist in solution in an alternative, partially autoinhibited conformation, which would convert into a fully active conformation upon interaction with a PIP_2/PS-containing membrane. Whether this represents another layer of regulation of RacGAP1 remains to be investigated.

An intriguing observation is that the truncated monomeric C1GAP construct, which has half as many membrane-binding surfaces and active sites as dimeric RacGAP1, binds to membranes as tightly as RacGAP1 and is more active on membranes. Since C1GAP and RacGAP1 are equally active in solution, it is unlikely that the N- and C-terminal regions exert an inhibitory effect on the GAP domain in RacGAP1. Alternatively, the difference could be due to the dimerization of RacGAP1. While all active sites in the C1GAP sample are, by construction, available, RacGAP1 can bind to the membrane (hence use its GAP domains) either one or both subunits at a time (Figure 7b), as observed previously for a dimeric ArfGEF (Das et al., 2019). This mechanism may enhance the ability of the unbound subunit to search for new Rac1-GTP substrates to inactivate on the membrane (reviewed in Nawrotek et al., 2023), eventually optimizing the full removal of Rac1 from the division plane. The role of dimerization remains an important question for RacGAP1, and more generally for membrane-peripheral proteins, which will require further investigation in future studies.

3.2 | The specificity of RacGAP1 for Rac1

Our study also reveals that the marked preference of RacGAP1 for Rac1 in solution is not modified by the presence of membranes. With a barely detectable activity towards Cdc42 (122-fold lower than Rac1) and a very weak activity towards RhoA (41-fold lower than Rac1) in the context of membranes, inactivation of Cdc42 and RhoA by RacGAP1 is thus likely negligible in cells with respect to Rac1.

Thus, whether in solution or on membranes, RacGAP1 has intrinsic determinants to efficiently inactivate Rac1, but not the Cdc42 or RhoA GTPases. This narrow specificity defines RacGAP1 as a Rac1-specific GAP and rules out that membranes function as modulators of RacGAP1 specificity. Our study identifies two residues involved in this specificity, one located in the switch 1 and the other in the insert helix. Based on the conformation of the switch 1 seen in Rac1-GDP-Pi, we propose that the unique Gly30 in the switch 1 of Rac1 allows the switch 1 to adopt an open conformation immediately following GTP hydrolysis, while Rac1-GDP-Pi is still bound to RacGAP1. By making fewer interactions with Pi compared to RhoA and Cdc42, Rac1 could thus release Pi faster than RhoA and Cdc42. In addition, as the switch 1 would have already converted to the open conformation of unbound Rac1-GDP, no further conformational change would be needed upon Rac1-GDP dissociation. Overall, Gly30 would thus lower the energy cost of the GAP reaction for Rac1, which can contribute to the specificity of RacGAP1. A second determinant is Lys132 in the insert region. Our converging biochemical results and structural modeling suggest that this residue is involved in both Rac1/RacGAP1 and Rac1/membrane interactions, both of which are important for defining the optimal spatial coincidence between Rac1 and RacGAP1 at the surface of the membrane (Figure 7a). They also point to a previously unnoticed role for the insert region in defining how Rac1 interacts with membranes. Finally, our model of the membrane-bound Rac1/RacGAP1 complex suggests that a third contribution to efficient GAP activity is provided by the polybasic geranylgeranylated C-terminus of Rac1. The lipidated C-terminus of GTPases is increasingly recognized as an important player in defining the orientation of small GTPases with respect to the membrane (reviewed in Hutchins & Gorfe, 2024). Its sequence is very different in Cdc42 and RhoA, which can lead to an orientation on the membrane that does not match that of RacGAP1. Together, we propose that the specificity of RacGAP1 for Rac1 on membranes involves a

combination of protein-nucleotide interactions at the switch 1, protein–protein interactions at the insert, and protein/membrane interactions at the insert region and the C-terminus, all of which depend on specific residues that differ between Rac1 and either Cdc42 or RhoA.

4 | CONCLUDING REMARKS

In conclusion, our biochemical study provides a robust mechanistic model for the specific inactivation of Rac1 by RacGAP1 during cytokinesis and provides a solid framework to interpret cell-based assays. This model is in agreement with cell biology studies that found that Rac1 is inactivated by RacGAP1 (Canman et al., 2008; Toure et al., 1998; Zhuravlev et al., 2017) and that suppression of Rac1 activity in the division plane is critical for successful cytokinesis completion (Yoshizaki et al., 2003, reviewed in Jordan & Canman, 2012). Why in some studies Rac1 appears to be insensitive to RacGAP1 or RhoA appears to be inactivated by RacGAP1 (Miller & Bement, 2009; Zhang & Glotzer, 2015) may thus be due to indirect effects. These indirect effects could involve the coupling between the regulatory machineries of Rac1 and RhoA at the membrane such as, for example, the interaction of RacGAP1 with the RhoA-specific GEF Ect2 (Zou et al., 2014). Finally, our findings point to potential new avenues for targeting RacGAP1 in cancer by small molecules. These could include protein-membrane inhibitors, as exemplified by Bragsin which inhibits the activation of Arf GTPases by impairing the orientation of a specific activator on membranes (Nawrotek et al., 2019), or inhibitors that target the unique properties of Rac1, such as the anti-metastatic inhibitor C41, which replaces the GDP nucleotide by exploiting the flexibility of the switch 1 (Dilasser et al., 2025).

5 | MATERIALS AND METHODS

5.1 | Protein expression and purification

Full-length human RacGAP1 carrying a 6xHis-MBP tag followed by a TEV protease cleavage site was cloned into the Gateway destination vector pHMGWA. The GAP domain (residues 348–546) and C1GAP (residues 283–546) constructs carrying a 6xHis tag followed by a TEV protease cleavage site were cloned into the Gateway destination vector pHGWA. All RacGAP1 constructs were expressed in *E. coli* BL21(DE3) in auto-induction LB medium supplemented with ampicillin at 100 μg/mL and $ZnSO_4$ at 10 μM. Cells were grown at 37°C and 200 rpm shaking to an OD_{600} of 0.8. Overexpression was induced overnight at 20°C. Bacterial cultures were centrifuged for 30 min at 4000×*g*. Bacterial pellets were resuspended in 4°C lysis buffer (50 mM HEPES, pH 7.5, 500 mM NaCl, 20 mM imidazole, 10 μM $ZnSO_4$, 2 mM DTT, 5% glycerol) containing a protease inhibitor cocktail, lysozyme at 0.25 mg/mL (Sigma-Aldrich) and 7.5 U/mL of benzonase (Sigma Aldrich) disrupted by sonication on ice. Lysates were spun down for 45 min at 20000×*g*. The cleared lysate supernatant was loaded onto a Ni-NTA affinity chromatography column (HisTrap FF, Cytiva), previously equilibrated with buffer A (50 mM HEPES, pH 7.5, 500 mM NaCl, 20 mM imidazole, 10 μM $ZnSO_4$, 2 mM DTT, 5% glycerol). His-tagged proteins were eluted with about 35 mM imidazole. The His-tags or the His_6-MBP tags were cleaved by TEV protease (1:20 w/w) in a dialysis bag with 10 kDa cut-off against 2 L of dialysis buffer (50 mM HEPES, pH 7.5, 250 mM NaCl, 10 μM $ZnSO_4$, 2 mM DTT, 5% glycerol) at 4°C overnight for the GAP and C1GAP constructs, or for 48 h for full-length RacGAP1. The cleaved fractions were separated using an affinity chromatography column (HisTrap FF, Cytiva) and further purified by gel filtration on a Superdex 200 16/600 column (Cytiva) equilibrated with storage buffer (50 mM HEPES, pH 7.5, 150 mM NaCl, 10 μM $ZnSO_4$, 2 mM DTT, 5% glycerol).

Human full-length Rac1, RhoA, and Cdc42 carrying a C-terminal 6-His tag were expressed and purified as in (Peurois et al., 2017). The Rac1 K132M mutant was generated by site-directed mutagenesis and obtained from GenScript. The Rac1 P29S mutant was obtained with the site-directed mutagenesis kit QuikChange II (Agilent). The Rac1 G30S, P29S, and K132M mutants were purified as in (Dilasser et al., 2025). Rac1 lacking the C-terminal residues ($Rac1^{1\text{-}177}$) was purified as in (Ferrandez et al., 2017).

The coumarin-labeled phosphate-binding protein (MDCC-PBP) was prepared and purified as described in (Solscheid et al., 2015).

Proteins' purity was assessed by SDS-PAGE.

5.2 | Liposome preparation and flotation assays

All liposomes were prepared as described in (Peurois et al., 2017). All lipids are from Avanti. The lipid composition of liposomes is given in Table S2. The size distribution of liposomes was controlled by dynamic light scattering. Liposome flotation experiments were performed as described in (Karandur et al., 2017). Proteins at a concentration of 2.0 μM were incubated for 15 min with liposomes at 1 mM (lipid concentration). Liposome-bound proteins (top fraction), unbound proteins (bottom fraction), and the middle fraction were collected and analyzed by SDS-PAGE. The fraction of liposome-bound proteins was estimated as the ratio of the top fraction to the total proteins. All experiments were done at least in duplicate.

5.3 | GAP kinetics assays

For GAP assays, small GTPases were pre-loaded with GTP as described in (Peurois et al., 2017). GAP kinetics were measured using a reagentless biosensor assay, which measures the increase in fluorescence of MDCC-PBP upon binding of inorganic phosphate (Solscheid et al., 2015). GTP hydrolysis reactions were carried out in HKM buffer (50 mM HEPES pH 7.5, 120 mM potassium acetate, 1 mM $MgCl_2$). GAP kinetics were monitored by fluorescence, recorded at $\lambda_{ex} = 430$ nm and $\lambda_{em} = 465$ nm, on a Cary Eclipse fluorimeter (Varian) under stirring or on a FlexStation plate reader. We noted that the fluorescence signal was quickly saturated in the presence of liposomes due to Pi contamination from phospholipids. The assays were thus optimized by removing Pi by addition of 0.004 mg/mL purine nucleoside phosphorylase and 0.06 mg/mL 7-methylguanosine to all solutions prior to dilutions as described (Brune et al., 1994). Small GTPases were at a concentration of 2.0 μM, MDCC-PBP at 10 μM. Except when indicated otherwise, the concentrations of the GAP domain, C1GAP and RacGAP1 ranged from 1 to 50 nM for the determination of k_{cat}/K_M in solution, from 0.1 to 1 nM for C1GAP in the presence of liposomes, and from 1 to 10 nM for full-length RacGAP1 in the presence of liposomes. Inactivation of RhoA was very slow and required GAP concentrations from 10 to 100 nM. For GAP assays in the presence of plasma membrane-like liposomes, the concentration of total lipids was 100 μM. MDCC-PBP was pre-incubated with liposomes for 2 min, then RacGAP1 constructs were added and the mixture was incubated for 2 more min before the GTP-loaded GTPases were added. k_{obs} values were obtained by fitting the kinetics curves to a single exponential equation. k_{cat}/K_M were determined by linear regression from k_{obs} values measured over a range of RacGAP1 constructs concentrations following the Michaelis–Menten formalism as described in (Galicia et al., 2019). Activation of Rac1 mutants was characterized using a single RacGAP1 concentration (10 nM in solution and at 0.1 nM on PML liposomes). For each Rac1 construct, GTP hydrolysis kinetics were measured simultaneously in the presence and in the absence of RacGAP1. To take into account the difference in spontaneous GTP hydrolysis of the mutants, the increase in GTPase activity was then expressed as the ratio between k_{obs} values for the C1GAP-catalyzed and the spontaneous hydrolysis rate.

5.4 | Gel filtration experiments

100 μL of purified proteins at 50–100 μM were injected on a Superdex S200 10/300 GL column, pre-equilibrated with the elution buffer containing 50 mM HEPES pH 7.5, 150 mM NaCl, 2 mM $MgCl_2$, and 2 mM β-mercaptoethanol.

5.5 | Rac1-GDP-Pi and Rac1-GDP structure determination

Crystallization screens were performed using the sitting-drop vapor diffusion method at 18 °C with a Mosquito robot (TTP LabTech) in 96-well crystallization plates by mixing 100 nL of Rac1(1–177)-GDP at 5 mg/mL with 100 nL of precipitant solution. Crystals of Rac1-GDP-Pi were obtained in the A2 condition from the PACT++HTS screen (Jena Bioscience) containing 100 mM succinic acid/sodium phosphate/glycine (SPG) buffer pH 5 and 25% PEG 1500. The Rac1-GDP crystals were obtained in the C11 condition from the PACT ++HTS (Jena Bioscience) containing 100 mM HEPES pH 7.0, 200 mM calcium chloride, and 20% PEG 6000. Crystals were cryo-protected using the reservoir solution supplemented with 20% glycerol prior to flash freezing. Complete diffraction datasets were collected on PROXIMA-2A beamline (SOLEIL synchrotron, France) (Rac1-GDP, resolution 1.8 Å) or ID30A (ESRF) (Rac1-GDP-Pi, resolution 2.27 Å) and were integrated with the program XDSme (https://code.google.com/archive/p/xdsme/). The resolution of the Rac1-GDP structure is 0.8 Å higher compared to our original Rac1-GDP structure (Ferrandez et al., 2017). The structures were solved by molecular replacement with CCP4 Phaser using the structure of Rac1-GDP as a model (Ferrandez et al., 2017) (PDB entry code 5N6O). Refinements were carried out with the program Phenix (Liebschner et al., 2019), in alternation with graphical building using Coot41. Data collections and refinements statistics are reported in Table S3. Coordinates and structure factors of Rac1-GDP and Rac1-GDP-Pi have been deposited in the Protein Data Bank with entry codes 8S1N and 8S1O.

5.6 | Structure modeling

The structure of the C1GAP tandem was predicted using Alphafold 3 (Krokidis et al., 2025). The prediction is of confident high quality, with a predicted local distance difference test (plDDT) between 100 and 80, and a predicted template modeling score (pTM), which measures the accuracy of the overall structure, of 0.86. Structures were aligned with Pymol from the Sbgrid Consortium. Docking of the Rac1-RacGAP1 model on membranes was done with the OPM/PPM web server (Lomize et al., 2022).

AUTHOR CONTRIBUTIONS

Pavlina Dubois: Methodology; data curation; formal analysis; writing – review and editing; investigation.

Yann Ferrandez: Data curation; formal analysis; writing – review and editing; methodology; investigation. **Clara Rey:** Investigation. **Cyril Pages:** Investigation. **Agata Nawrotek:** Writing – review and editing; investigation; funding acquisition; conceptualization; methodology; formal analysis; project administration; supervision; validation. **Jacqueline Cherfils:** Writing – review and editing; writing – original draft; funding acquisition; formal analysis; project administration; supervision; conceptualization; investigation; validation.

ACKNOWLEDGMENTS

Agata Nawrotek was supported by a grant from the French National Research Agency (ANR-22-CE11-0004); Jacqueline Cherfils was supported by grants from the Fondation pour la Recherche Médicale (EQU202003010344) and the French National Research Agency (ANR-18-0013-02) and by the Grand Prix Jungfleisch of the French Academy of Sciences. We thank Marie-Hélène Kryzske (Cherfils lab) for her help with the statistical analysis. We thank the scientific staff at the SOLEIL (Gif-sur-Yvette, France) and ESRF (Grenoble, France) synchrotrons for their help and support with the X-ray crystallography experiments. Open access publication funding provided by COUPERIN CY26.

CONFLICT OF INTEREST STATEMENT

The authors declare no competing interests.

DATA AVAILABILITY STATEMENT

Coordinates and structure factors of the X-ray crystallography structure of Rac1-GDP and Rac1-GDP-Pi have been deposited in the Protein Data Bank under accession codes PDB ID: 8S1N and PDB ID: 8S1O.

ORCID

Agata Nawrotek https://orcid.org/0000-0001-7708-6381

REFERENCES

Amin E, Jaiswal M, Derewenda U, Reis K, Nouri K, Koessmeier KT, et al. Deciphering the molecular and functional basis of RHOGAP family proteins: a systematic approach toward selective inactivation of rho family proteins. J Biol Chem. 2016;291:20353–71.

Basant A, Glotzer M. A GAP that divides F1000Res 6 1788.2018 spatiotemporal regulation of RhoA during cytokinesis. Curr Biol. 2017;28:R570–80.

Bastos RN, Penate X, Bates M, Hammond D, Barr FA. CYK4 inhibits Rac1-dependent PAK1 and ARHGEF7 effector pathways during cytokinesis. J Cell Biol. 2012;198:865–80.

Bigay J, Gounon P, Robineau S, Antonny B. Lipid packing sensed by ArfGAP1 couples COPI coat disassembly to membrane bilayer curvature. Nature. 2003;426:563–6.

Brune M, Hunter JL, Corrie JE, Webb MR. Direct, real-time measurement of rapid inorganic phosphate release using a novel fluorescent probe and its application to actomyosin subfragment 1 ATPase. Biochemistry. 1994;33:8262–71.

Canagarajah B, Coluccio Leskow F, Ho JYS, Mischak H, Saidi LF, Kazanietz MG, et al. Structural mechanism for lipid activation of the Rac-specific GAP, β2-Chimaerin. Cell. 2004;119:407–18.

Canman JC, Lewellyn L, Laband K, Smerdon SJ, Desai A, Bowerman B, et al. Inhibition of Rac by the GAP activity of centralspindlin is essential for cytokinesis. Science. 2008;322:1543–6.

Cherfils J, Zeghouf M. Regulation of small GTPases by GEFs, GAPs, and GDIs. Physiol Rev. 2013;93:269–309.

Das S, Malaby AW, Nawrotek A, Zhang W, Zeghouf M, Maslen S, et al. Structural organization and dynamics of Homodimeric Cytohesin family Arf GTPase exchange factors in solution and on membranes. Structure. 2019;27:1782–1797 e1787.

Dilasser F, Rose L, Quemener A, Ferrandez Y, Hassoun D, Rousselle M, et al. A Rac-specific competitive inhibitor of guanine nucleotide binding reduces metastasis in triple-negative breast cancer. Cell Rep Med. 2025;6:102233.

Duellberg C, Auer A, Canigova N, Loibl K, Loose M. In vitro reconstitution reveals phosphoinositides as cargo-release factors and activators of the ARF6 GAP ADAP1. Proc Natl Acad Sci U S A. 2021;118:e2010054118.

Ferrandez Y, Zhang W, Peurois F, Akendengue L, Blangy A, Zeghouf M, et al. Allosteric inhibition of the guanine nucleotide exchange factor DOCK5 by a small molecule. Sci Rep. 2017;7:14409.

Fullbrunn N, Nicastro R, Mari M, Griffith J, Herrmann E, Rasche R, et al. The GTPase activating protein Gyp7 regulates Rab7/Ypt7 activity on late endosomes. J Cell Biol. 2024;223:e202305038.

Galicia C, Lhospice S, Varela PF, Trapani S, Zhang W, Navaza J, et al. MglA functions as a three-state GTPase to control movement reversals of Myxococcus xanthus. Nat Commun. 2019;10:5300.

Hirshberg M, Stockley RW, Dodson G, Webb MR. The crystal structure of human rac1, a member of the rho-family complexed with a GTP analogue. Nat Struct Biol. 1997;4:147–52.

Hutchins CM, Gorfe AA. From disorder comes function: regulation of small GTPase function by intrinsically disordered lipidated membrane anchor. Curr Opin Struct Biol. 2024;87:102869.

Jaffe AB, Hall A. Rho GTPases: biochemistry and biology. Annu Rev Cell Dev Biol. 2005;21:247–69.

Jantsch-Plunger V, Gönczy P, Romano A, Schnabel H, Hamill D, Schnabel R, et al. Cyk-4: a rho family Gtpase activating protein (gap) required for central spindle formation and cytokinesis. J Cell Biol. 2000;149:1391–404.

Jordan SN, Canman JC. Rho GTPases in animal cell cytokinesis: an occupation by the one percent. Cytoskeleton (Hoboken). 2012;69:919–30.

Karandur D, Nawrotek A, Kuriyan J, Cherfils J. Multiple interactions between an Arf/GEF complex and charged lipids determine activation kinetics on the membrane. Proc Natl Acad Sci U S A. 2017;114:11416–21.

Karimzadeh F, Primeau M, Mountassif D, Rouiller I, Lamarche-Vane N. A stretch of polybasic residues mediates Cdc42 GTPase-activating protein (CdGAP) binding to phosphatidylinositol 3,4,5-trisphosphate and regulates its GAP activity. J Biol Chem. 2012;287:19610–21.

Kawashima T, Hirose K, Satoh T, Kaneko A, Ikeda Y, Kaziro Y, et al. MgcRacGAP is involved in the control of growth and differentiation of hematopoietic cells. Blood. 2000;96:2116–24.

Krauthammer M, Kong Y, Ha BH, Evans P, Bacchiocchi A, McCusker JP, et al. Exome sequencing identifies recurrent somatic RAC1 mutations in melanoma. Nat Genet. 2012;44:1006–14.

Krokidis MG, Koumadorakis DE, Lazaros K, Ivantsik O, Exarchos TP, Vrahatis AG, et al. AlphaFold3: an overview of applications and performance insights. Int J Mol Sci. 2025;26:3671.

Lekomtsev S, Su KC, Pye VE, Blight K, Sundaramoorthy S, Takaki T, et al. Centralspindlin links the mitotic spindle to the plasma membrane during cytokinesis. Nature. 2012;492:276–9.

Liebschner D, Afonine PV, Baker ML, Bunkoczi G, Chen VB, Croll TI, et al. Macromolecular structure determination using X-rays, neutrons and electrons: recent developments in Phenix. Acta Crystallogr D Struct Biol. 2019;75:861–77.
Lomize AL, Todd SC, Pogozheva ID. Spatial arrangement of proteins in planar and curved membranes by PPM 3.0. Protein Sci. 2022; 31:209–20.
Miller AL, Bement WM. Regulation of cytokinesis by rho GTPase flux. Nat Cell Biol. 2009;11:71–7.
Minoshima Y, Kawashima T, Hirose K, Tonozuka Y, Kawajiri A, Bao YC, et al. Phosphorylation by aurora B converts MgcRacGAP to a RhoGAP during cytokinesis. Dev Cell. 2003;4:549–60.
Mishima M, Kaitna S, Glotzer M. Central spindle assembly and cytokinesis require a kinesin-like protein/RhoGAP complex with microtubule bundling activity. Dev Cell. 2002;2:41–54.
Mishra AK, Lambright DG. High-throughput assay for profiling the substrate specificity of Rab GTPase-activating proteins. Methods Mol Biol. 2021;2293:27–43.
Molt RW Jr, Pellegrini E, Jin Y. A GAP-GTPase-GDP-P (i) intermediate crystal structure analyzed by DFT shows GTP hydrolysis involves serial proton transfers. Chemistry. 2019;25: 8484–8.
Murayama K, Kato-Murayama M, Hosaka T, Kitamura T, Yokoyama S, Shirouzu M. Structural basis for the effects of Ser387 phosphorylation of MgcRacGAP on its GTPase-activating activities for CDC42 and RHOA. J Struct Biol. 2024; 216:108151.
Nawrotek A, Benabdi S, Niyomchon S, Kryszke MH, Ginestier C, Caneque T, et al. PH-domain-binding inhibitors of nucleotide exchange factor BRAG2 disrupt Arf GTPase signaling. Nat Chem Biol. 2019;15:358–66.
Nawrotek A, Dubois P, Zeghouf M, Cherfils J. Molecular principles of bidirectional signalling between membranes and small GTPases. FEBS Lett. 2023;597:778–93.
Nixon AE, Brune M, Lowe PN, Webb MR. Kinetics of inorganic phosphate release during the interaction of p21ras with the GTPase-activating proteins, p120-GAP and neurofibromin. Biochemistry. 1995;34:15592–8.
Padovani D, Folly-Klan M, Labarde A, Boulakirba S, Campanacci V, Franco M, et al. EFA6 controls Arf1 and Arf6 activation through a negative feedback loop. Proc Natl Acad Sci U S A. 2014;111: 12378–83.
Pan H, Guan R, Zhao R, Ou G, Chen Z. Mechanistic insights into central spindle assembly mediated by the centralspindlin complex. Proc Natl Acad Sci U S A. 2021;118:e2112039118.
Pasqualato S, Cherfils J. Crystallographic evidence for substrate-assisted GTP hydrolysis by a small GTP binding protein. Structure. 2005;13:533–40.
Pavicic-Kaltenbrunner V, Mishima M, Glotzer M. Cooperative assembly of CYK-4/MgcRacGAP and ZEN-4/MKLP1 to form the centralspindlin complex. Mol Biol Cell. 2007;18:4992–5003.
Peurois F, Veyron S, Ferrandez Y, Ladid I, Benabdi S, Zeghouf M, et al. Characterization of the activation of small GTPases by their GEFs on membranes using artificial membrane tethering. Biochem J. 2017;474:1259–72.
Rittinger K, Walker PA, Eccleston JF, Smerdon SJ, Gamblin SJ. Structure at 1.65 a of RhoA and its GTPase-activating protein in complex with a transition-state analogue. Nature. 1997;389: 758–62.
Solscheid C, Kunzelmann S, Davis CT, Hunter JL, Nofer A, Webb MR. Development of a Reagentless biosensor for inorganic phosphate, applicable over a wide concentration range. Biochemistry. 2015;54:5054–62.
Sondermann H, Soisson SM, Boykevisch S, Yang SS, Bar-Sagi D, Kuriyan J. Structural analysis of autoinhibition in the Ras activator son of sevenless. Cell. 2004;119:393–405.
Stebbins CE, Galan JE. Modulation of host signaling by a bacterial mimic: structure of the salmonella effector SptP bound to Rac1. Mol Cell. 2000;6:1449–60.
Toure A, Dorseuil O, Morin L, Timmons P, Jegou B, Reibel L, et al. MgcRacGAP, a new human GTPase-activating protein for Rac and Cdc42 similar to drosophila rotundRacGAP gene product, is expressed in male germ cells. J Biol Chem. 1998;273:6019–23.
Wadsworth P. The multifunctional spindle midzone in vertebrate cells at a glance. J Cell Sci. 2021;134:jcs250001.
White EA, Glotzer M. Centralspindlin: at the heart of cytokinesis. Cytoskeleton (Hoboken). 2012;69:882–92.
Wurtele M, Wolf E, Pederson KJ, Buchwald G, Ahmadian MR, Barbieri JT, et al. How the Pseudomonas aeruginosa ExoS toxin downregulates Rac. Nat Struct Biol. 2001;8:23–6.
Yoshizaki H, Ohba Y, Kurokawa K, Itoh RE, Nakamura T, Mochizuki N, et al. Activity of rho-family GTPases during cell division as visualized with FRET-based probes. J Cell Biol. 2003;162:223–32.
Zhang D, Glotzer M. The RhoGAP activity of CYK-4/MgcRacGAP functions non-canonically by promoting RhoA activation during cytokinesis. Elife. 2015;4:e08898.
Zhuravlev Y, Hirsch SM, Jordan SN, Dumont J, Shirasu-Hiza M, Canman JC. CYK-4 regulates Rac, but not rho, during cytokinesis. Mol Biol Cell. 2017;28:1258–70.
Zou Y, Shao Z, Peng J, Li F, Gong D, Wang C, et al. Crystal structure of triple-BRCT-domain of ECT2 and insights into the binding characteristics to CYK-4. FEBS Lett. 2014;588:2911–20.

SUPPORTING INFORMATION

Additional supporting information can be found online in the Supporting Information section at the end of this article.

How to cite this article: Dubois P, Ferrandez Y, Rey C, Pages C, Nawrotek A, Cherfils J. The cytokinesis regulator RacGAP1 is a Rac1-specific GAP on membranes. Protein Science. 2026;35(3):e70488. https://doi.org/10.1002/pro.70488